

Illustrating motion through DLP Photography

Sanjeev J. Koppal
Carnegie Mellon University
koppal@cs.cmu.edu

Srinivasa G. Narasimhan
Carnegie Mellon University
srinivas@cs.cmu.edu

Abstract

Strobe-light photography creates beautiful high-frequency effects by capturing multiple object copies. Single-chip DLP projectors produce a similar effect, with two important distinctions. Firstly, strobing occurs at different frequencies: at 10000 Hz, due to the DMD chip, and at 120Hz, due to the colorwheel. Secondly, DLP illumination lacks the perception of 'on-off' flashing that characterizes a strobe-light, since these frequencies are beyond human perception. Deblurring images taken under such strobe-like illumination is difficult, especially for articulated and deformable objects, since the deconvolution kernel can be different at each pixel. Instead we process DLP photographs to create new images that either summarize a dynamic scene or illustrate its motion. We conclude by discussing the frequencies present in DLP photographs, comparing them to images taken under skylight and fluorescent light.

1. The DMD-Colorwheel effect

Historically, imaging dynamic scenes proved to be challenging. Motion blur removes interesting detail, resulting in smeared images. Objects move in and out of focus while exhibiting appearance changes. Keeping the scene framed correctly on the object requires accurate control of the camera pose. In addition, image quality and object speed trade-off against one another. Today's high-speed cameras, although relatively expensive, have the frame rate and pixel resolution to address these issues for most applications.

However, there are still reasons to capture a single image of a fast moving scene. Summarizing a dynamic event is one application: for example, photographers may capture the aggressive posturing of two competitors in a sport. Another use is for experiments that do not justify the expense of a high speed camera, such as ballistics for a bullet passing through some material. Finally, high-speed photographs have aesthetic value and are used by artists to capture dynamic and complex scenes such as moving liquids and breaking glass ([14],[26]). In Figure 1 we show one of many photographs taken by Harold Edgerton ([9]) who used a high-speed strobe light to obtain many copies of moving objects. Figure 1(a) explains that the fast flickering of the strobe light creates multiple copies of the moving object. A similar effect is possible using the illumination of DLP (Digital Light Processing) projectors.

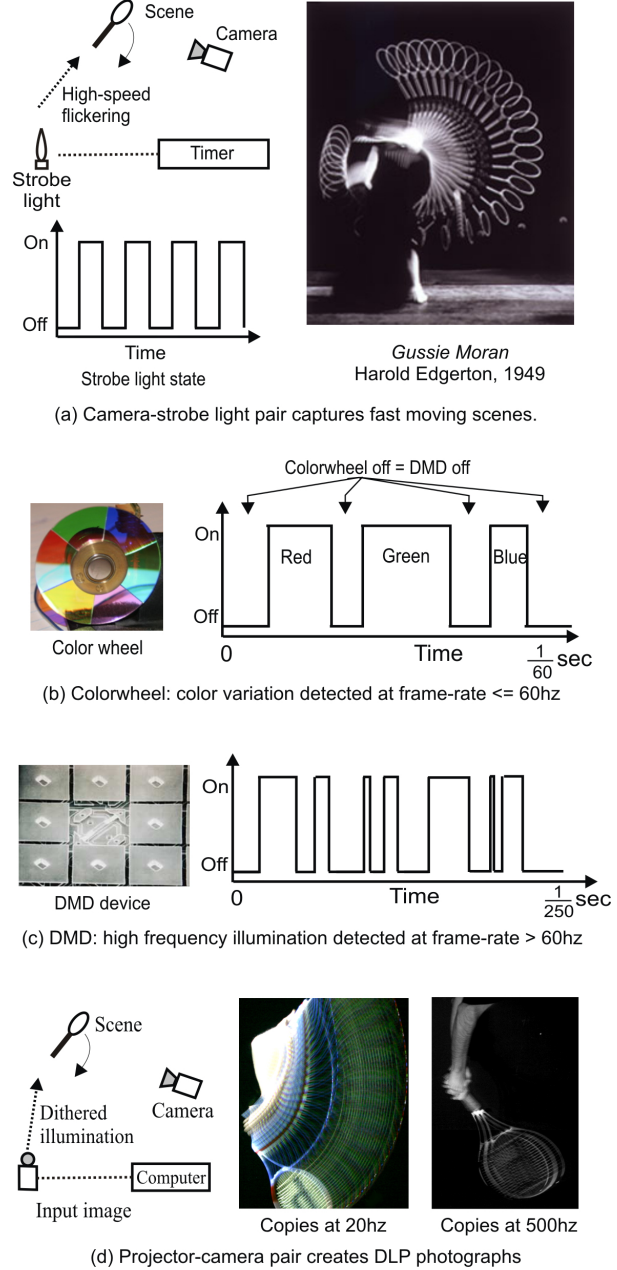


Figure 1. Photographing fast moving scenes with varying illumination: In (a) we show Edgerton's setup, which photographed moving scenes without motion blur using a strobe light. Strobe-light photography produces high-frequency object 'copies'. In (b) we show our setup with an unsynchronized DLP projector illuminating the scene. Both the projector's DMD and its color wheel produce a similar strobe-like effect which we term the DMD-colorwheel effect, as shown in (d).

Every single-chip DLP projector contains two important components: a DMD (Digital Micromirror Device) device and a color wheel. The DMD chip modulates the projected light after it is reflected off an array of 10×10 micron mirrors ([3]). Any displayed intensity is made up of pulses of light created by these mirrors switching on and off. The MEMS mirrors can change their binary state within 10^{-6} of a second, resulting in crisp images with sharp contrast. Since a DMD device modulates light, it can only create binary images. In comparison, even the fastest LED strobe lights have a ramp-up time, creating grayscale values.

Projecting color images involves synchronized control between the DMD chip and the color wheel, which rotates at 120Hz and is divided into red, green and blue filters. The 'rainbow effect' of the color wheel is well-known to display researchers who wish to remove or reduce it ([18],[10],[19],[25], [7], [17], [13]). Many researchers even remove the color wheel to increase the projector contrast in their experiments ([11], [1]). Instead of treating this effect as a problem that must be compensated for, our work demonstrates that DLP illumination can be exploited to photograph dynamic scenes.

In Figure 1 we illustrate how both these components create strobing effects for different classes of moving scenes. We term this the **DMD-Colorwheel effect**. For example, commercial cameras (which operate around 60Hz) cannot detect the high frequency dithering of the DMD chip and, instead, the colorwheel effect will dominate for most dynamic scenes, as shown in Figure 1(b). Note that the region of zero intensity in between the color pulses are due to the mirrors on the DMD devices turned off.

For higher frame rate cameras, we can detect the dithered illumination within each color pulse, as in Figure 1(c). Therefore DLP illumination can produce strobing effects for both real-time and high-speed scenes. This is illustrated in 1(d), where we image a tennis racket being swung. With a regular camera, the number of copies is large, and they are captured under different illumination (red, green and blue). In contrast, the copies in the photograph taken with a high-speed camera are fewer and grayscale.

DLP photographs offer two alternatives to the problem of deblurring images with deformable and articulated objects. First, a dynamic scene can be summarized by combining many DLP photographs. Second, videos can be created from DLP photographs that, although not deblurred, still give the perception of motion. For example, in some cases, the RGB channels in a DLP image can illustrate movement. We also discuss the frequencies present in DLP photographs, comparing them to images taken under both skylight and fluorescent illumination. Finally, we demonstrate that DLP illumination is programmable at each pixel. This is an advantage over similar camera aperture methods that can only control the shutter speed globally.

1.1. Related work

Talbot ([24]) created the first flash photography of dynamic scenes in 1851 using an electric spark. This technique was further improved on by Worthington ([28]), but was limited to scenes that did not cause much motion blur. In 1930 Edgerton ([4]) invented the first xenon flash tube and started creating truly high-speed strobe images as in Figure 1(a). Current LED strobe-lights have replaced the original xenon tube and can be computer controlled. As far as the authors are aware, DLP projectors have not been used widely for creating strobe-light photography.

Instead, DLP projectors have become popular in recent years in the vision and graphics communities. The temporal dithering or flickering of the DMD device changes too quickly to be noticed by humans, and so it was exploited in interactive and virtual office space applications to encode structured light ([21], [2]). Since then much related work has emerged such as reengineering a DLP projector for programmable imaging ([16]), calibrating the temporal dithering for high-speed active lighting ([15]). DMD devices have also been used separately for reconstruction ([6]), (dynamic scene relighting ([27], [12]) and 3D displays ([8]).

2. Formation of DLP photographs

Consider a scene, as in Figure 2, consisting of a moving opaque object O illuminated by a strobing distant light source $S(t)$ of frequency $\frac{1}{f}$. For the sake of simplicity, let us assume the object moves with uniform velocity in a plane with constant depth, and the optical flow of the projection of O on the image, O_{proj} is $\vec{V} = (u, v)$. The longest dimension of the object's image along \vec{V} is D . The scene is imaged by a pin-hole camera C whose exposure time is T . If $E(x, y, t)$ is the scene radiance incident at pixel (x, y) at time t , then the measured image is:

$$I(x, y) = \int_{t=0}^T E(x, y, t) S(t) dt \quad (1)$$

Since $S(t)$ is the Dirac comb of frequency $\frac{1}{f}$, we can simplify the above integration into a summation. We further separate $E(x, y, t)$ into a sum of the background radiance and the object radiance:

$$I(x, y) = \Sigma_{o=0}^{\omega} O(x, y, t_o) + \Sigma_{b=0}^{\beta} B(x, y, t_b) \quad (2)$$

Here t_o and t_b are time indices for when the radiance is due to object and background respectively. Since we are interested in scenes containing fast moving objects, $\omega \ll \beta$. To prevent the background from dominating the measured intensity, our experiments are conducted in a dark room and therefore $B(x, y, t) = 0$. This is not a strict constraint and we note that with a camera of sufficiently high dynamic

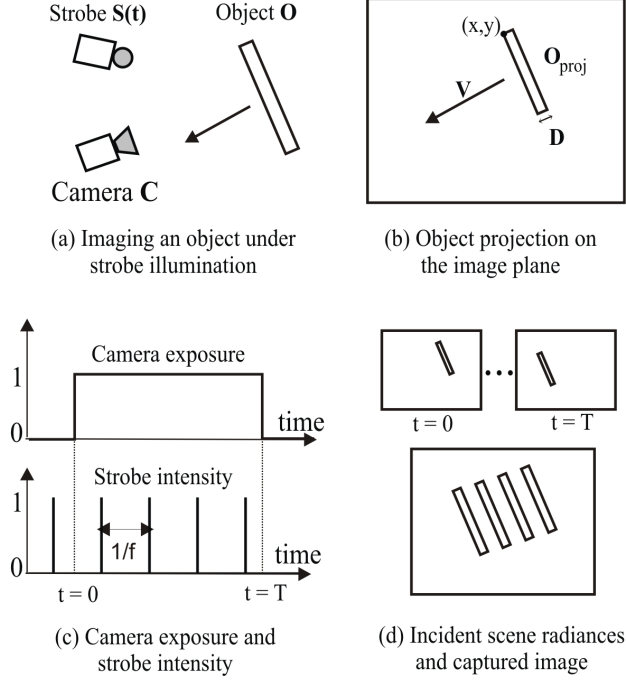


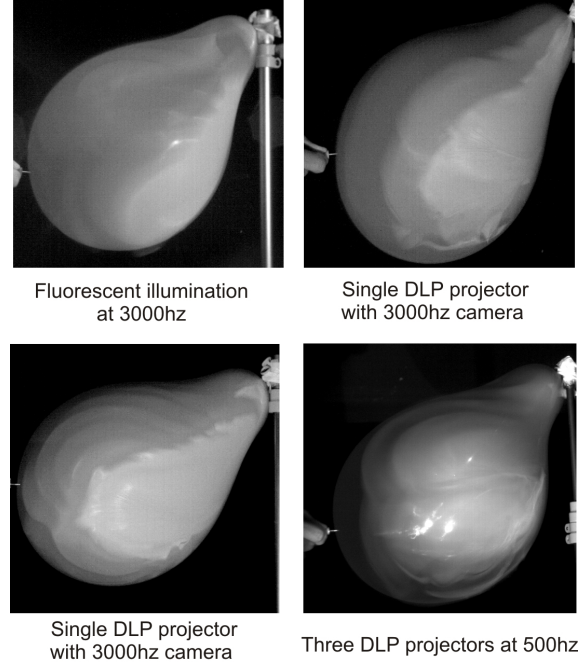
Figure 2. **Image formation model:** Consider a scene illuminated with a strobing light source, as in (a). Let an object move in a plane parallel to the image plane and at constant velocity, as in (b). Since the illumination is a dirac comb, the photograph can be modeled as a dot-product between a video of a moving object with the illumination, as in (c). The number of photographs is determined by the camera exposure, producing an image, (d).

range, this would not be necessary. The image formation equation now becomes:

$$I(x, y) = \sum_{o=0}^{\omega} O(x, y, t_o) \quad (3)$$

To get an image containing many copies of the object, we would like to eliminate motion blur. Let the edge of the object be imaged at pixel (x, y) as in Figure 2. To prevent motion blur, the optical flow of O_{proj} must cover a distance D in time $\frac{1}{f}$. Therefore the speed of the flow must be Df and $\|\vec{V}\| = \sqrt{u^2 + v^2} = Df$. If the pin-hole camera has focal length F and if the object moves in a plane at depth Z then the actual speed of the object is $\frac{DZf}{F}$.

The DMD chip has a frequency of a 10^6 Hz, but the dithering in a commercial projector occurs at around $f = 10000$ Hz ([15]). If the ratio $\frac{Z}{F} = 100$, the longest dimension D is 0.0001 inch, then the actual speed of the object is 100 feet per second. This is approximately the case for an air balloon bursting as showing in Figure 3. Under fluorescent lighting, viewed at 1000fps, the balloon is smeared in a single frame, and this high-speed event is lost. However, when viewed under DLP illumination, the images at 1000fps show copies of the edge of the balloon. We used an

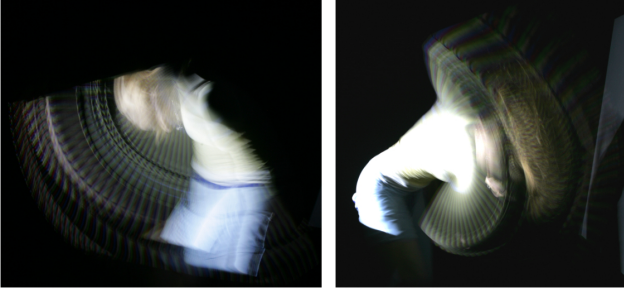


Strobing effect due to DMD at high-speeds

Figure 3. **DLP photographs of a bursting balloon:** An air balloon bursting can be captured fully using a 10000hz camera. In (a) we show what happens when the event is captured under fluorescent illumination, with a lesser rate of 3000hz. In one frame the event is lost in motion blur. In (b) we show images taken under 3000hz, but this time with DLP illumination. Notice the multiple copies of edge of balloon as it moves. We are able to capture images of this high-speed event, due to the temporal dithering of the DMD device in the projector. Similarly in (c) we use three DLP projectors, which are not synchronized. We are able to capture the balloon bursting at 500hz.

Infocus In38 projector projecting a plain gray image of intensity 192 of 3000 lumens, viewed by a Photron PCI-1024 high-speed camera. Our setup enables photography of an event occurring at 10 times the frame rate of the viewing camera. Next, we use three projectors that are unsynchronized creating a higher strobing frequency and therefore obtaining a similar photograph at a lower frame rate of 500Hz.

The color wheel has a frequency of around 120Hz, and if we image a scene whose longest dimension D is 0.001 inch then the object speed must be at least 12 feet per second. This is approximately the case for fast human movements. In Figure 4 we show pictures of a tabla (hand drum) being played, as well as a ballet dancer performing. Note that some of the copies appear at different colors, since they are illuminated when the color wheel turns the red, green or blue filters.



Two poses of a ballet dancer



Close-ups of tabla drumming Side-view of tabla drumming

Figure 4. **Selected DLP photographs:** We photographed two artists, a ballet dancer and a tabla (hand drum) player, under DLP illumination. Both activities are 'real time' and the color wheel effect dominates the images. The camera exposure was 1 second.

2.1. Separation of strobed image component

DLP photographs consists of two components. The first is due to the strobe effect of the light source and is created by the objects that move at a speed greater than or equal to $\frac{DZf}{F}$. We call this component the strobed component since it contains multiple object copies. The other parts of the image consist of pixels that have motion blur, which we call the non-strobed component. We wish to segment out the interesting high-frequency strobed component of the DLP photograph since these describe the motion.

To achieve this separation we make certain assumptions which may seem restrictive, but in practice, we obtain good results. First, we assume that the albedo of the object is constant and variation due to shading is negligible. This is the same premise made in structured light, where scene points on the light stripe show an intensity maxima despite their different surface normals and BRDF. Second, we assume that every pixel is either strobed or non-strobed, and we wish to find the mask $\alpha(x, y) \in \{0, 1\}$ such that:

$$I(x, y) = \alpha(x, y) I_b(x, y) + (1 - \alpha(x, y)) I_{nb}(x, y) \quad (4)$$

where I_b and I_{nb} are the blurred and non-blurred images respectively.

Separation for DMD strobing: A well-known method of blur identification ([22],[29],[23]) is to threshold the measured intensities. From Equation 3 we note that the

strobed component would consist of a single scene radiance, whereas a non-strobed component would contain more. We use the mean of the measured intensities as a threshold. In Figure 5 we do this for a photograph of a tennis racket taken at 125Hz. Note that errors only happen when specularities occur since this violates our assumption of constant BRDF.

Separation for color wheel strobing: In this case, the regions of the image that are strobed have a dominant color (R, G or B). In contrast, the slower moving parts of the image have the normal distribution of RGB. Therefore the color channel mean is less for strobed regions than non-strobed regions. Once again, we use this mean as a threshold to create a mask for separation, as seen in Figure 5.

3. Summarizing fast events

An image summarizing a video sequence can be created by stitching important frames together, as in shape-time photography ([5]). However, the object must move slowly since otherwise motion blur will render the final result difficult to interpret. DLP photographs summarize a short burst of action, since they contain multiple copies of moving objects. Applying a similar method as shape-time photography to a collection of DLP photographs creates a summary image for fast motion.

In Figure 6(a) we show images created by processing a volume of DLP photographs of a tabla player. We first separate the images into the strobed and non-strobed part. Except for the first image, the rest of the images are strobed. The top image is created by taking the intensity maxima of each pixel over all the photographs, which produces the effect of combining the different copies and gives a summary of the motions that occurred. In contrast, the bottom of Figure 6(a) is creating by masking the high intensity portions of each image and pasting them on top of each other. Instead of blending the outputs, these summaries enforce an order into the images.

We can also create an impression of the scene's motion by blending the intensities of the different DLP photographs as in the top of Figure 4. Since each DLP photograph is already a summary of some part of the scene motion, we are able to compress a long and fast dynamic motion into a simple, pleasing summary. We show the mask-blending results for the ballet dancer in Figure 6(b). Since the scale of the scene is larger, the DLP effect is only observed in a frustum of illumination, which could be corrected by placing additional projectors (these may be too bright for the dancer, but may be fine for other objects). In this case, the order and number of the scene matters, since there is a lot of overlap in the original images, and these were chosen by the user.

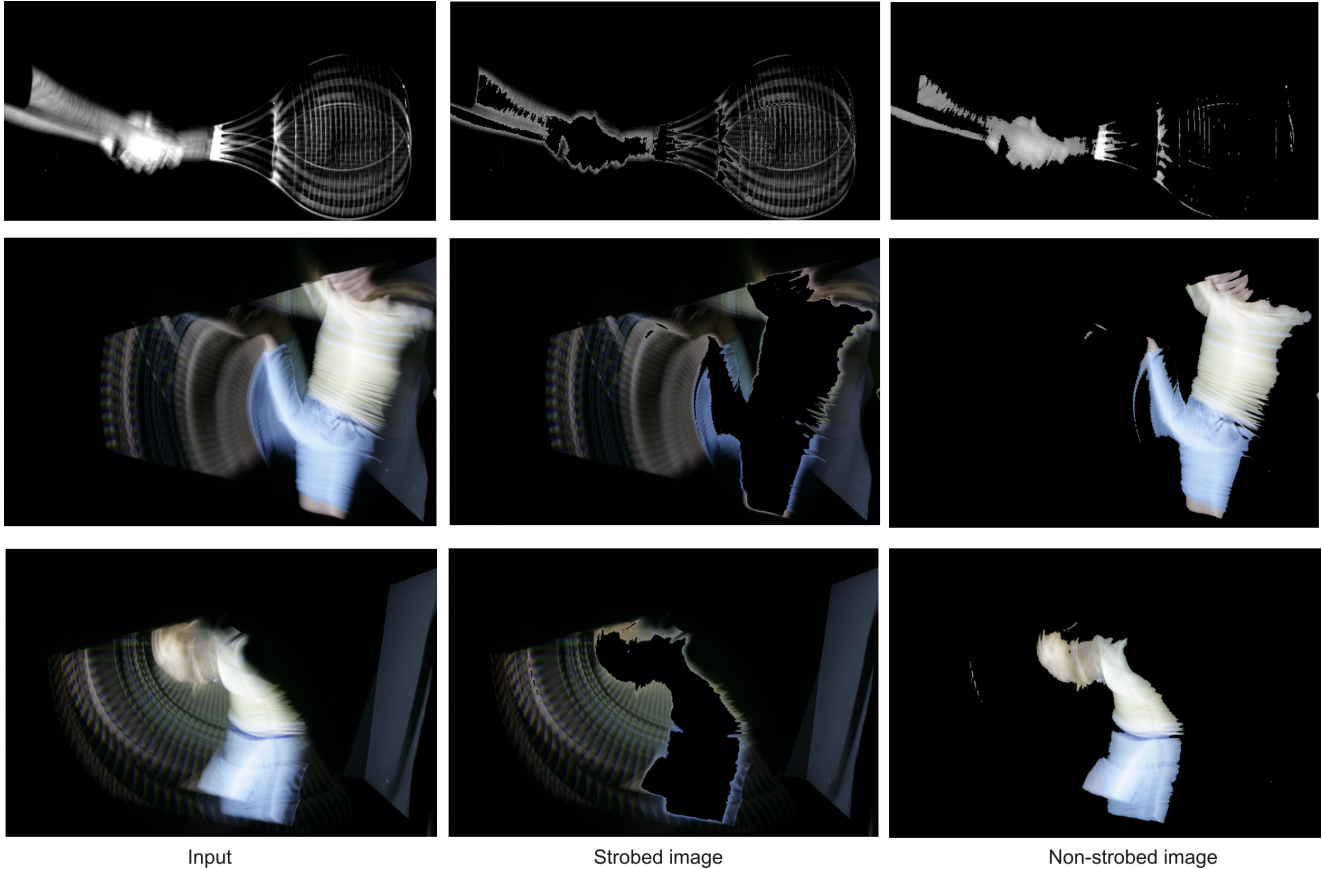


Figure 5. **Separating strobed and non-strobed components:** We use a simple appearance model to separate the strobed component of a scene: since the faster parts of the scene are imaged for a shorter time, their intensity is lower than other parts of the scene. This works especially well for the color wheel examples shown in the last two rows, where each strobed component is illuminated by either R, G or B light and has approximately a third of its original intensity.

4. Creating the illusion of motion

Here we present three ways of processing a set of DLP photographs to produce a video that illustrates a scene’s motion. We do not claim to deblur the scene or recover the motion in a quantifiable fashion. Instead, we believe these motion illustrations contain more information than the set of photographs by themselves and provide an easy way to visualize the event that occurred. The trade-off is that each of these techniques produces good results in certain broad classes of scenes, and may fail for others.

Blending: In Figure 7 (a) we show the first three frames of a motion illustration video for the ballet dancer. The frames in this video were created by differentially alpha blending the strobed and non-strobed components of DLP photographs taken at 1s exposure. The non-strobed component were blended slowly, at 10% per frame. In contrast, the strobed component was blended quickly, at 50% per frame. Since the strobed component naturally contains the fast moving parts of the scene, this gives the impression of motion.

Color demultiplexing: In Figure 7 (b) we show pictures of a tabla (hand drum) musician playing under DLP illumination. Due to the color-wheel effect, the different object copies are colored in a repeated series of red, green and blue. Each image can be demultiplexed into three grayscale images, tripling the frame-rate. Cycling the RGB copies gives the impression of motion only when the speed of the object is close to the frequency of the colorwheel (120Hz), resulting in fewer object copies and unlike the ballet photographs. This method works best when the objects in the scene are themselves close to grayscale: objects with significant red, green or blue components will be imaged darkly or not at all in the complement illumination.

Segmentation: In Figure 7 (c) we create a video from an image from Figure 3 by thresholding the image intensities. Since the balloon parts that move first are replaced by the black background, these are least bright. Therefore the balloon shrinks from the outer edge inwards. This segmentation approach produces a believable result for a convex object, such as a balloon, since the image center is brighter than the outer edge.



Image created by pixel maximum of all DLP photographs

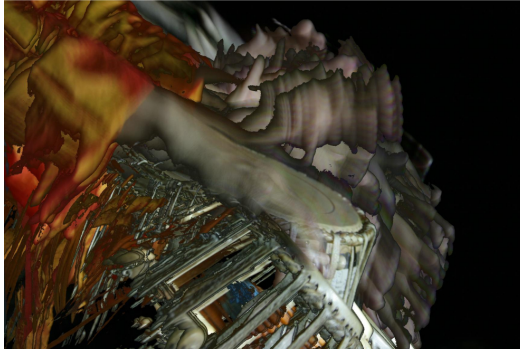


Image created by combining masked DLP photographs
(a) Tabla player summaries



Image created by pixel maximum of all DLP photographs



Image created by combining masked DLP photographs
(b) Ballet dancer summaries

Figure 6. Motion summaries: By combining DLP photographs in different ways we can summarize events. For both the tabla player, (a), and the ballet dancer, (b), we show summaries created by taking pixel maxima as well as by masking and superimposing the images. In the maxima case, no image ordering exists and all edges are blended. In the masking case, image order matters and edges exist between different stages of the action.

5. Discussion: Deblurring photographs of dynamic scenes

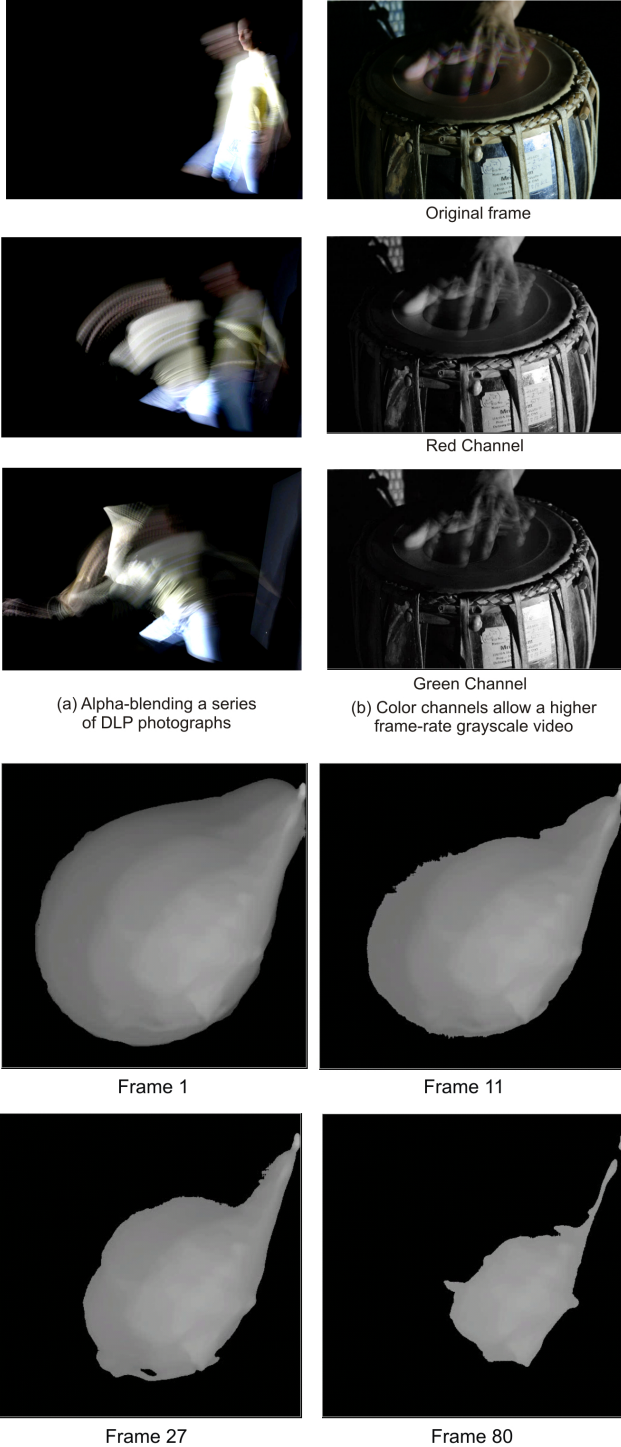
In this section we conclude by analyzing the frequency space of images taken under DLP illumination. One important goal in vision and graphics is to deblur scenes containing complex motion such as articulated and deformable objects. Since this is challenging, most work has focused instead on deblurring the image when a global kernel or point spread function (PSF) can be assumed for the image as a whole. In the previous sections, we avoid the problem of deblurring by instead creating visual content that either summarizes the scene dynamics or gives the perception of object motion.

In Figure 8(a)-(c), we show images taken under DLP, skylight and fluorescent illumination. The object is a cardboard sheet translating from left to right with the PSF approximated by a small white dot placed on the sheet. We use this as a good starting point for blind deconvolution methods. For skylight and fluorescent light, we also tried the 'box' PSF which assumes constant incident illumination during exposure. Note that the best deconvolution occurs with the DLP photograph. In Figure 8(d) we show the frequencies of the PSFs. Note that the highest frequencies are due to the DLP illumination. Although previous work has either used camera apertures to create similar images ([20]) or shown some deblurring results ([15]), we are the first to analyze and compare the frequencies in DLP illumination.

For future work, we would like to explore an advantage of DLP illumination over camera aperture control methods, which is the ability to program the aperture for each pixel. For example, in Figure 9 we show a balloon bursting at 10000Hz, illuminated by a striped pattern. Since each pattern dithers at a different rate, parts of the balloon are illuminated as it explodes. This should allow applications for deblurring of very fast scenes, where the deblurring kernel varies over the image.

References

- [1] Q. Chen and T. Wada. A light modulation/demodulation method for real-time 3d imaging. *3D digital imaging and modeling*, 2005. 2
- [2] D. Cotting, M. Naef, M. Gross, and H. Fuchs. Embedding imperceptible patterns into projected images for simultaneous acquisition and display. *ISMAR*, 2004. 2
- [3] D. Dudley, W. Duncan, and J. Slaughter. Emerging digital micromirror device (dmd) applications. *Proc. of SPIE*, 4985, 2003. 2
- [4] H. Edgerton. Strobe photography: A brief history. *Optical engineering*, 1984. 2
- [5] W. Freeman and H. Zhang. Shape-time photography. *CVPR*, 2003. 4



(c) Intensity gradients allow a grayscale video from a single image

Figure 7. Different types of motion illustrations: We present three types of motion illustrations for DLP photographs. In (a), we differentially blend the strobed and non-strobed components. In (b) we triple the effective frame-rate by separating the RGB image components, exploiting the effect of the color wheel. Finally in (c), we apply segmentation to convex objects to reconstruct the fast event. Please see supplementary material for better visualization.

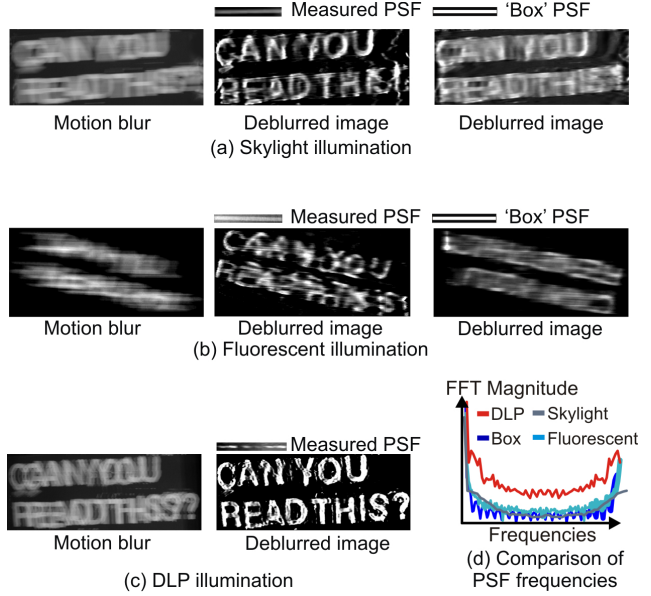


Figure 8. DLP photographs contain higher frequencies compared to other types of illumination: In (a) and (b) we show deconvolution results with skylight and fluorescent illumination. The blind deconvolution algorithm was given the intensity profile of a white dot as a starting point. The result for deblurring the same motion under DLP illumination (c) can be read easily. Analysis of frequencies in the recovered PSF shows DLP illumination preserves high frequency information.

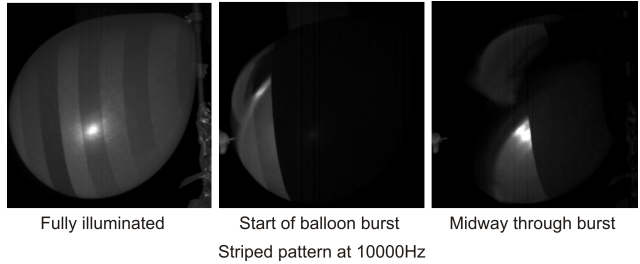


Figure 9. DLP illumination as a programmable aperture: On the left we show a balloon illuminated by a striped pattern from a DLP projector. Each stripe dithers at a different rate. We show two instances just after the balloon is burst, showing the edge of the contracting balloon in two different positions. If the pattern was uniformly set to either the first or second stripe value, one of these events would have been missed.

- [6] M. Fujigaki, Y. Morimoto, and Q. Gao. Shape and displacement measurement by phase-shifting scanning moire method using digital micro-mirror device. In *Intl. conf. on experimental mechanics*, volume 4537, 2001. 2
- [7] T. Jarvenpaa. Measuring color breakup of stationary images in field-sequential-color displays. *Journal of the Society for Information Display*, 2005. 2
- [8] A. Jones, I. McDowall, H. Yamada, M. Bolas, and

- P. Debevec. Rendering for an interactive 360 degree light field display. In *ACM SIGGRAPH*, 2007. 2
- [9] G. Kayafas and E. Jussim. Stopping time: The photographs of harold edgerton. *Abrams*, 2000. 1
- [10] S. Kima, T. Shibataa, T. Kawaia, and K. Ukaib. Ergonomic evaluation of a field-sequential colour projection system. *Displays*, 2007. 2
- [11] J. Lee, S. Hudson, J. Summet, and P. Dietz. Moveable interactive projected displays using projector based tracking. *Symposium on User Interface Software and Technology*, 2005. 2
- [12] I. McDowall and M. Bolas. Fast light for display, sensing and control applications. In *IEEE VR Workshop on Emerging Display Technologies*, 2005. 2
- [13] M. Mori, T. Hatada, K. Ishikawa, T. Saishoji, O. Wada, J. Nakamura, and N. Terashima. Mechanism of color breakup in field-sequential-color projectors. *Journal of the Society for Information Display*, 1999. 2
- [14] E. Muybridge, H. Edgerton, and J. Shaw. Time/motion. *Dewi Lewis Publishing*, 2004. 1
- [15] S. G. Narasimhan, S. J. Koppal, and S. Yamazaki. Temporal dithering of illumination for fast active vision. *ECCV*, 2008. 2, 3, 6
- [16] S. K. Nayar, V. Branzoi, and T. Boulton. Programmable imaging using a digital micromirror array. *IEEE CVPR*, 2004. 2
- [17] K. I. O. Wada, J. Nakamura and T. Hatada. Analysis of color breakup in field-sequential color projection system for large area displays. *Display Workshops*, 1999. 2
- [18] M. Ogata, K. Ukai, and T. Kawai. Visual fatigue in congenital nystagmus caused by viewing images of color sequential projectors. *Display Technology*, 2005. 2
- [19] O. Packer, L. Diller, J. Verweij, B. Lee, J. Pokorny, D. Williams, D. Dacey, and D. H. Brainard. Characterization and use of a digital light projector for vision research. *Vision Research*, 2001. 2
- [20] R. Raskar, A. Agrawal, and J. Tumblin. Coded exposure photography: Motion deblurring using fluttered shutter. *ACM SIGGRAPH*, 2006. 6
- [21] R. Raskar, G. Welch, M. Cutts, A. Lake, L. Stesin, and H. Fuchs. The office of the future: A unified approach to image-based modeling and spatially immersive displays. *SIGGRAPH*, 1998. 2
- [22] S. Reeves and R. Mersereau. Blur identification by the method of generalized cross-validation. *Transactions on image processing*, 1992. 4
- [23] A. Rosenfeld and A. Kak. Digital image processing. *New York Academic*, 1982. 4
- [24] W. H. F. Talbot. Note on instantaneous photographic images. *Philosophical magazine*, 1851. 2
- [25] E. Umezawa, T. Shibata, T. Kawai, and K. Ukai. Ergonomic evaluation of the projector using color-sequential display system. *45th Annual Congress of the Japan Ergonomics Assoc.*, 2004. 2
- [26] M. Waugh. Liquid sculptures. *www.liquidsculpture.com*, 2004. 1
- [27] A. Wenger, A. Gardner, C. Tchou, J. Unger, T. Hawkins, and P. Debevec. Performance relighting and reflectance transformation with time-multiplexed illumination. *ACM SIGGRAPH*, 2005. 2
- [28] A. M. Worthington. A study of splashes. *Longman green*, 1908. 2
- [29] Y. You and M. Kaveh. A regularization approach to joint blur identification and image restoration. *Transactions on image processing*, 1996. 4